

Pulse-controlled quantum gate sequences on a strongly coupled qubit chain

Holger Frydrych,^{1,*} Michael Marthaler,² and Gernot Alber¹

¹*Institut für Angewandte Physik, Technische Universität Darmstadt, D-64289 Darmstadt*

²*Institut für Theoretische Festkörperphysik, Karlsruhe Institute of Technology (KIT), 76131 Karlsruhe, Germany*

(Dated: December 3, 2024)

We propose a selective dynamical decoupling scheme on a chain of permanently coupled qubits, which is capable of dynamically suppressing any coupling in the chain by applying sequences of local pulses to the individual qubits. We demonstrate how this pulse control can be used to implement a sequence of quantum gates on the chain which entangles all the qubits. We find that high entanglement fidelities can be achieved as long as the total number of coupled qubits is not too large. We discuss the applicability of our model specifically for superconducting flux qubits which can be strongly coupled to allow for the fast implementation of two-qubit gates. Since dynamically modifying the couplings between flux qubits is challenging, they are a natural candidate for our approach.

PACS numbers: 03.67.Pp, 03.67.Lx, 85.25.Cp

I. INTRODUCTION

Current implementations of qubits are typically either well isolated from noise, but difficult to couple, or strongly coupled, but difficult to isolate. To achieve the goal of building a working quantum computer for the tasks of quantum simulation and, eventually, quantum computation, we require an architecture that is capable of strongly coupling qubits to implement fast multi-qubit gates, but that can also isolate qubits from each other and the environment when no gate operation is performed.

In quantum optics, extensive work has been done using trapped ions or atoms as qubits, and scalable architectures that can trap and address a large number of qubits simultaneously exist [1]. These qubits feature excellent coherence times, yet the implementation of two-qubit gates in these architectures is still a topic of ongoing research, although recently promising proposals were made in this regard [2–4].

Likewise, we have seen significant progress in solid state qubit architectures [5–7], and there exist promising candidates for scalable systems. Gate-defined spin qubits [8, 9] feature excellent coherence properties [10], but coupling two qubits remains a challenge despite proposals for efficient coupling [11, 12]. For superconducting qubits, both indirect coupling via a resonator [13] and direct capacitive coupling of detuned qubits [14] have been demonstrated and are comparatively easy to realize. Recently, good coherence properties were achieved for flux qubits [15], a particular type of superconducting qubit with a very large anharmonicity. This anharmonicity allows them to be strongly coupled [16], which makes them particularly interesting for the implementation of fast two-qubit gates. However, their tunability is limited by the need for an optimal operating point, which makes it difficult to isolate the qubits when no gate operation

should be performed.

In this article, we attempt to overcome the isolation problem of flux qubits and other similarly strongly coupled qubit systems by an alternative ansatz. We study a qubit chain with always present nearest-neighbor couplings and make use of a pulse generator to exert external control on the qubits with the aim of suppressing unwanted qubit couplings. We demonstrate in numerical simulations that this simple pulse control enables us to implement a sequence of entangling gate operations on the qubit chain to entangle all the qubits in the chain in a GHZ state [17] with high fidelity. We thus show that a system of strongly coupled flux qubits may be used for universal quantum computation purposes without the need to control the qubit couplings.

Our pulse control is based on dynamical decoupling [18], which is a generalization of techniques developed in the nuclear magnetic resonance community [19–22]. It makes use of external control pulses being applied in rapid succession to the system in question. With a carefully designed control sequence it is possible to eliminate (parts of) a Hamiltonian interaction up to a certain order. Dynamical decoupling has been successfully implemented in numerous experiments to protect qubit states from the effects of decoherence [23–27]. For our purposes, we are interested in selectively decoupling only certain interactions between qubits while keeping others alive, a possibility proposed already by Viola *et al.* [28]. A particularly simple to handle subset of decoupling schemes applicable to networks of qubits employs only Pauli pulses to individual qubits. Several different construction methods for such Pauli operator schemes exist [29–33]. In dynamical decoupling, it is typically assumed as a first approximation that the applied control pulses are instantaneous and unitary. In our numerical calculations, we go beyond this approximation by simulating realistic pulse lengths.

The paper is organized as follows: In Sec. II we present the physical model of our flux qubit chain and the type of control we have over the system. Section III recapit-

*Electronic address: holger.frydrych@physik.tu-darmstadt.de

ulates the basic principles of dynamical decoupling and demonstrates how we can decouple a single and a pair of qubits from the rest of the chain. In Sec. IV we then look at the concrete implementation of a two-qubit entangling gate, and we estimate the achievable gate fidelity with the help of numerical simulations. Finally, in Sec. V we use this gate to entangle the qubits in our chain and present numerical simulations on the achievable state fidelity depending on the number of qubits in the chain.

II. THE COUPLED QUBIT SYSTEM MODEL

We consider a system of N qubits in a chain with nearest-neighbor couplings described by the Hamiltonian ($\hbar = 1$)

$$H_0 = \sum_{i=1}^N \left[\epsilon_i \sigma_z^{(i)} / 2 + f_i(t) \sigma_x^{(i)} \cos(\omega t + \varphi_i(t)) \right] - g \sum_{i=1}^{N-1} \sigma_x^{(i)} \sigma_x^{(i+1)}, \quad (1)$$

where the $\sigma_a^{(i)}$ are the Pauli operators applied to the i -th qubit, and ϵ_i are the qubits' eigenenergies. The coupling between the qubits is assumed to be uniform and characterized by the coupling strength g . The effects of the pulse generator (frequency ω) on each individual qubit are governed by the time-dependent pulse amplitudes $f_i(t)$ and the phases $\varphi_i(t)$. This model is strongly inspired by a system of coupled flux qubits [16], where the pulse generator is a microwave emitter. However, alternative qubit designs exist which are also described by this model.

Transforming the Hamiltonian (1) into the rotating frame with the unitary operator $U_\omega = \exp(i\omega \sum_i \sigma_z^{(i)} t / 2)$, the coupled N -qubit chain is governed by the Hamiltonian

$$H = U_\omega H_0 U_\omega^\dagger = \frac{1}{2} \sum_{i=1}^N \left[\Delta_i \sigma_z^{(i)} + f_i(t) \left(e^{i\varphi_i(t)} \sigma_+^{(i)} + e^{-i\varphi_i(t)} \sigma_-^{(i)} \right) \right] - \frac{g}{2} \sum_{i=1}^{N-1} \left[\sigma_x^{(i)} \sigma_x^{(i+1)} + \sigma_y^{(i)} \sigma_y^{(i+1)} \right], \quad (2)$$

where $\sigma_\pm = \frac{1}{2}(\sigma_x \pm i\sigma_y)$. The $\Delta_i = \epsilon_i - \omega$ indicate the discrepancy between the individual qubits' eigenenergies and the frequency of the driving field and should ideally be zero.

III. DECOUPLING INDIVIDUAL AND PAIRS OF QUBITS

Our goal is to exploit the strong coupling which can be implemented between e.g. flux qubits [16] for a fast

high-fidelity two-qubit gate operation. To this end, it is necessary that the two qubits on which the gate operation is performed are temporarily isolated from the surrounding qubits. Traditionally, this would require switching off the interactions of the two qubits with their neighbors, but this process is complicated and often limits the achievable interaction strength g . Instead, we will employ dynamical decoupling to cancel the effects of individual couplings as needed.

In dynamical decoupling, the natural evolution of the N -qubit chain under the acting Hamiltonian H is periodically interrupted by strong and short control pulses applied to the system. As a first approximation to be revised later, we will treat these control pulses as instantaneous unitary operators p_j , which are applied to our chain of qubits at times $j\tau$. By introducing the unitary operators $g_j = p_j p_{j-1} \cdots p_0$, the resulting time evolution $U(t)$ after M pulses can be written as

$$U(M\tau) = p_M e^{-iH\tau} p_{M-1} \cdots p_1 e^{-iH\tau} p_0 = g_M \left(g_{M-1}^\dagger e^{-iH\tau} g_{M-1} \right) \cdots \left(g_0^\dagger e^{-iH\tau} g_0 \right) = g_M e^{-ig_{M-1}^\dagger H g_{M-1} \tau} \cdots e^{-ig_0^\dagger H g_0 \tau}. \quad (3)$$

The operator g_M is arbitrary and is henceforth assumed to be $\mathbb{1}$ by an appropriate choice of the final decoupling pulse p_M . It is now possible to define an average Hamiltonian \bar{H} which leads to the same time evolution after the time $M\tau$, i.e.,

$$U(M\tau) \equiv e^{-i\bar{H}M\tau}. \quad (4)$$

By performing a Magnus expansion [34], the average Hamiltonian \bar{H} is expanded in powers of the pulse distance τ , i.e.,

$$\bar{H} = \bar{H}^{(0)} + \bar{H}^{(1)} + \bar{H}^{(2)} + \dots, \quad (5)$$

where the lowest order is found to be

$$\bar{H}^{(0)} = \frac{1}{M} \sum_{j=0}^{M-1} g_j^\dagger H g_j. \quad (6)$$

Our goal is to selectively remove couplings between specific qubit pairs in the lowest order $\bar{H}^{(0)}$ of the average Hamiltonian and to keep all others. We call a set of M operators $\{g_j\}_{j=0}^{M-1}$ a decoupling scheme if it fulfills this purpose. Note that the higher orders of \bar{H} are typically non-zero and remain as errors. However, their dependence on the pulse distance τ can be exploited to decrease their influence on the system dynamics. In the simplest case, the operators of a decoupling scheme can be repeated several times. If the total evolution time $M\tau$ is kept constant, this means that the distance τ between pulses is reduced, and so are the higher orders of the average Hamiltonian. However, while in theory a pulse distance of $\tau \rightarrow 0$ would be ideal, this only holds if the employed pulses are perfect and instantaneous. In our

scenario, we will run simulations with finite pulses. In these cases, choosing τ too small may actually be detrimental since we introduce additional errors into the system which may outweigh those we intend to correct.

More sophisticated decoupling strategies exist that can further eliminate certain higher orders. A particular example is the symmetrized dynamical decoupling (SDD) sequence which eliminates all the odd orders in the Magnus expansion of \bar{H} , thus achieving second order decoupling [35]. A symmetrized version of a decoupling scheme $\{g_j\}_{j=0}^{M-1}$ consists of $2M$ operators which are chosen as

$$g'_j = \begin{cases} g_j & \text{for } j < M, \\ g_{2M-1-j} & \text{for } j \geq M. \end{cases} \quad (7)$$

We will investigate the performance of both symmetrized and non-symmetrized decoupling strategies.

A. Decoupling an individual qubit

According to Eq. (1), the couplings in our qubit chain are always present. This means that in order to prevent the state of a single qubit from evolving requires work. If we do nothing, the qubit will interact with its immediate neighbors, changing the state of the system. By using dynamical decoupling, we can keep a single qubit isolated and its current state protected without having to switch off the interactions with the neighboring qubits.

It is a well-known result in dynamical decoupling that the state of a single qubit can be protected by an alternating XY pulse sequence. To protect a specific qubit i in the chain, we need to apply pulses of the form

$$p_j = \begin{cases} \sigma_x^{(i)} & \text{if } j \text{ is even,} \\ \sigma_y^{(i)} & \text{if } j \text{ is odd,} \end{cases} \quad (8)$$

which produces the decoupling operators (up to global phases)

$$\begin{aligned} g_0 &= \sigma_x^{(i)} & g_1 &= \sigma_z^{(i)} \\ g_2 &= \sigma_y^{(i)} & g_3 &= \mathbb{1}. \end{aligned} \quad (9)$$

Substituting these into Eq. (6), one can verify that this choice eliminates all the terms of the Hamiltonian (2) involving qubit i in the lowest order of the average Hamiltonian. Since the order of the operators g_j does not influence the lowest order $\bar{H}^{(0)}$, a YX pulse sequence has the same effect.

B. Decoupling a pair of qubits

In order to implement a two-qubit gate on a specific pair of qubits, it is necessary to isolate these two qubits from their neighboring qubits without affecting the interaction between the qubit pair. A simple extension of the

single-qubit decoupling scheme can achieve the desired effect. Specifically, to decouple the pair of qubits i and $i+1$ from the rest of the chain, we use pulses of the form

$$p_j = \begin{cases} \sigma_x^{(i)} \sigma_x^{(i+1)} & \text{if } j \text{ is even,} \\ \sigma_y^{(i)} \sigma_y^{(i+1)} & \text{if } j \text{ is odd.} \end{cases} \quad (10)$$

By calculating $\bar{H}^{(0)}$ in Eq. (6) for this particular choice of decoupling pulses, we can work out that the coupling between qubits i and $i+1$ remains unaffected, but the couplings between qubits $i-1$ and i and $i+1$ and $i+2$ are removed, as are the eigenenergy offsets $\Delta_i \sigma_z^{(i)}$ and $\Delta_{i+1} \sigma_z^{(i+1)}$. This decoupling sequence was found and studied in detail in [33], where also a more general sequence was presented to protect arbitrary two-qubit interactions. However, for our model and the subsequent discussion this simple sequence is already sufficient.

C. Combined decoupling on the whole qubit chain

The presented sequences can naturally be extended to the whole chain in such a way that we can choose which of the two-qubit couplings we want to keep and which we want to eliminate in the lowest order. Additionally, all of the eigenenergy terms $\Delta_i \sigma_z^{(i)}$ will be eliminated from $\bar{H}^{(0)}$. To achieve this, we apply alternating XY pulses to each qubit, just like in subsection III A, but we vary the order of the pulses. Two neighboring qubits whose interaction should be kept intact will have the same ordering. For those qubits for which the coupling is to be eliminated, the pulse order will be reversed. For example, if we wanted to protect the interaction between the first and last qubit pairs on a 5-qubit chain, but eliminate the couplings with the middle qubit, we would use the following pulse sequence:

$$\begin{aligned} p_0 &= \sigma_x^{(1)} \sigma_x^{(2)} \sigma_y^{(3)} \sigma_x^{(4)} \sigma_x^{(5)} \\ p_1 &= \sigma_y^{(1)} \sigma_y^{(2)} \sigma_x^{(3)} \sigma_y^{(4)} \sigma_y^{(5)} \\ p_2 &= p_0 \\ p_3 &= p_1. \end{aligned} \quad (11)$$

D. Symmetrized decoupling scheme

Applying the construction in Eq. (7) to the decoupling operators in Eq. (9), we can symmetrize our decoupling scheme. To implement the symmetrized scheme, we need to replace the pulse sequence $XYXY$ with the sequence $XYXIIIXYX$, with I the identity operator. The approach of subsection III C still works, so we can interchange the order of the X and Y pulses as needed. This pulse sequence achieves second-order decoupling and should therefore perform better in practice. However, since more pulses are required, faster pulses will be needed to implement this sequence.

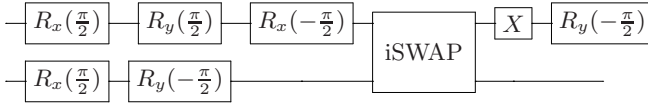


FIG. 1: The quantum circuit to implement a CNS gate with the help of the iSWAP gate and a number of single-qubit rotations.

IV. IMPLEMENTING THE TWO-QUBIT CNS GATE WITH DECOUPLING

In the following, we investigate how to implement an entangling two-qubit gate for the type of interaction present in our model. We look at how the necessary operations can be performed with the type of control that we can exert on our qubit chain. We also look at numerical simulations to determine the achievable fidelities and explore the scalability of our approach.

A. The CNS gate

The coupling between the qubits according to Eq. (1) is of XX type. Schuch and Siewert [36] studied natural gate operations resulting from such an interaction. They showed that, after an interaction time $T = \pi/(2g)$, this type of coupling produces a unitary iSWAP gate:

$$U_{\text{iSWAP}} := \exp \left[iT \frac{g}{2} \left(\sigma_x^{(i)} \sigma_x^{(i+1)} + \sigma_y^{(i)} \sigma_y^{(i+1)} \right) \right]. \quad (12)$$

This gate, like the better known SWAP gate, exchanges the state of two qubits, but introduces an additional phase on the swapped qubit states.

With the addition of a number of single-qubit gates, it is possible to use the iSWAP gate to implement the so-called CNS gate, which is a concatenation of a CNOT and a SWAP gate. This means that the CNS gate, just like the regular CNOT gate, is an entangling gate, which makes it particularly interesting. It is thus the entangling gate which is most easily implemented with the given XX -type coupling. The gate sequence depicted in Fig. 1 implements a CNS gate with the upper qubit being the control qubit. In this sequence, $X := \sigma_x$, and $R_a(\phi) := \exp(-i\sigma_a\phi/2)$ is a rotation around the axis a , which can be implemented with the help of the pulse generator. In order to implement the iSWAP gate, the two qubits must be decoupled from their neighbors for an interaction time $T = \pi/(2g)$.

B. Implementing the single-qubit gates

The required single-qubit gates consist entirely of rotations around the X and Y axes. They can be implemented with the help of the pulse generator by an appropriate choice of the parameter functions $f_i(t)$ and $\varphi_i(t)$

for each qubit i . The curve $f_i(t)$ describes the pulse shape, while $\varphi_i(t)$ can be used to select the direction of the rotation. The simplest pulse shape for our purposes is a rectangular pulse, so that the $f_i(t)$ are essentially binary functions, which take at any time either the value 0 or the value f . Here, f is the maximal pulse amplitude that can be implemented in the experimental setup. In contrast, a value of 0 means that the generator is switched off for this particular qubit.

To implement the rotation $R_x(\pi/2)$ on qubit i , we set $f_i(t) = f$ and $\varphi_i(t) = 0$ for a duration of $T = \pi/(2f)$. For the rotation in negative direction, $R_x(-\pi/2)$, we set $\varphi_i(t) = \pi$ instead. For the rotations around the Y axis, $R_y(\pm\pi/2)$, the appropriate value for the angle is $\varphi_i(t) = \pi/2$ for the positive rotation and $\varphi_i(t) = 3\pi/2$ for the negative rotation. Finally, to implement the X gate, we set $f_i(t) = f$ and $\varphi_i(t) = 0$ for a duration of $T = \pi/f$.

The gates can be implemented in parallel where possible, since the driving fields can be manipulated for each qubit individually without affecting the other qubits. However, the implementation of the pulses is disturbed by the qubit couplings and the eigenenergy shifts in the Hamiltonian (2). In order to achieve high-fidelity single-qubit gates, we have to ensure that the pulses are sufficiently fast, meaning $f \gg g$ and $f \gg \Delta_i$.

C. Implementing the iSWAP gate

In order to implement the iSWAP gate, we just need to let the natural interaction between the two qubits evolve for a time $T = \pi/(2g)$. During this time, the qubits need to be decoupled from the rest of the chain, which we accomplish with the decoupling sequence described in Sec. III B. To this effect, we need to implement σ_x and σ_y pulses on the two involved qubits. To implement σ_x on qubit i , we choose $f_i(t) = f$ and $\varphi_i(t) = 0$ for a time duration $T = \pi/f$, to implement σ_y we choose $\varphi_i(t) = \pi/2$ instead.

As there are four operators g_i in our decoupling sequence, our time distance between pulses is $\tau = \pi/(8g)$. This means that, in order to implement the decoupling sequence, we require as an absolute minimum $f \geq 8g$. The implementation of the pulse takes the time π/f , for the remainder of the time $\tau - \pi/f$ we let the system evolve freely, i.e. $f_i(t) = 0$. If the pulse amplitude f is sufficiently large, it becomes possible to implement longer decoupling sequences, including the SDD sequence, to improve the decoupling efficiency further.

D. Physical limits and numerical simulations

In theory, it is advantageous to have a pulse amplitude f as large as possible. This would decrease the implementation time of both the single-qubit gates and the decoupling operators, resulting in a higher fidelity of the full gate operation. Additionally, sufficiently fast decoupling

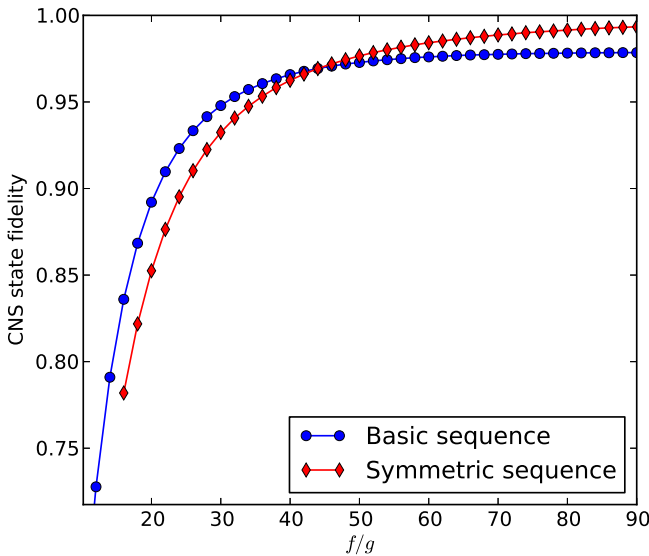


FIG. 2: (Color online) Achievable fidelity for a single CNS gate depending on the pulse amplitude f . Fidelity was calculated on a 6-qubit chain for the reduced state of the two gate qubits.

pulses would allow us to implement higher-order decoupling sequences, which would improve the fidelity even further. Unfortunately, there is a physical limit for f . If f is larger than the anharmonicity of the level structure, there is a possibility that the driving field may excite states beyond the first excited state in our qubit model, therefore invalidating the two-state approximation.

We use numerical simulations to determine the fidelity of the CNS gate operation which can be achieved as a function of the maximal pulse amplitude f . For this purpose, we simulated a qubit chain with varying numbers of qubits N , where all qubits are initially prepared in the ground state $|0\rangle$. Only qubit i is prepared in the superposition $(|0\rangle + |1\rangle)/\sqrt{2}$, where qubit i is chosen to be close to the middle of the chain. The gate operation is then performed on qubits i and $i + 1$, and the resulting density operator ρ is calculated for the whole qubit chain. In the final step, we take a partial trace to get the reduced density operator for qubits i and $i + 1$, ρ_{gate} , and calculate the state fidelity \mathcal{F} as the overlap with the expected state, $|\Psi\rangle = (|00\rangle + |11\rangle)/2$,

$$\mathcal{F} = \left| \sqrt{\langle \Psi | \rho_{\text{gate}} | \Psi \rangle} \right| \quad (13)$$

The fidelity is virtually independent of the number N of qubits for $N > 3$, but depends strongly on f . Figure 2 shows results obtained from the numerical simulations for a chain with $N = 6$ qubits, assuming that there are no eigenenergy shifts ($\Delta_i = 0$). The first plot (blue circles) shows the results for the basic decoupling sequence from Sec. III B. It is apparent that the fidelity

rises quickly with increasing f/g and reaches $\mathcal{F} \geq 0.9$ at about $f = 20g$. At about $f = 60g$ the fidelity approaches the asymptotical limit of instantaneous pulses. Note that these results are achieved by just four decoupling pulses. To improve on the asymptotic limit, a more sophisticated decoupling strategy is required. The second plot (red diamonds) shows results from the symmetrized scheme described in Sec. III D. It requires twice as many decoupling operations and performs worse than the basic scheme for $f \leq 40g$. However, for sufficiently high pulse amplitudes it surpasses the basic scheme, and at $f \sim 75g$ it reaches a fidelity ≥ 0.99 . Additional improvements to the decoupling procedure might be possible via Eulerian decoupling [37] or by embedding decoupling schemes [38].

In experimental implementations, one possibility to achieve a high f/g ratio is to have a rather small coupling constant g . Let us consider as a concrete example two coupled superconducting qubits of the transmon type, which only feature a small anharmonicity and thus severely limit the pulse amplitude f . We might be able to realize a driving pulse of the order of $f \approx 200$ MHz, which would require the qubit coupling g to be smaller than 10 MHz to achieve a ratio $f/g = 20$. This would lead to rather slow two qubit gates, and much faster two-qubit gates have already been achieved using the X-mon architecture [39]. As an alternative we may consider superconducting flux qubits, which feature a much larger anharmonicity. This would allow for driving pulses of the order of several GHz. Flux qubits with always-on couplings of the order of 500 MHz were realized in [16], which would allow for fast two-qubit gates. However, even for flux qubits, achieving f/g ratios of 40 or bigger without weakening the qubit couplings or exciting higher states will be challenging. In order to overcome this limitation, it is advisable to look beyond the simple rectangular pulse shapes which were used in our simulations. More sophisticated self-correcting (to second order) pulse shapes have been proposed [40] which can significantly improve the fidelity of a single X or Y pulse and thus can compensate for a smaller pulse amplitude. Alternate proposals exist to design pulses which are less likely to excite higher states, thus enabling the use of a stronger pulse amplitude [41].

V. CREATING AN ENTANGLED GHZ STATE

As a practical example for our control model, we are going to use the CNS gate to entangle the qubits in our qubit chain. The qubits in the chain are initially prepared in the ground state $|0\rangle$. One of the qubits in the middle of the chain is then brought into the superposition state $(|0\rangle + |1\rangle)/\sqrt{2}$ by application of a Hadamard gate, which in our control model can be implemented as an X gate followed by a rotation $R_y(-\pi/2)$. One application of the CNS gate to this qubit and its neighbor will entangle the two qubits. Additional applications of the CNS gate then allow us to entangle the remaining qubits in the chain,

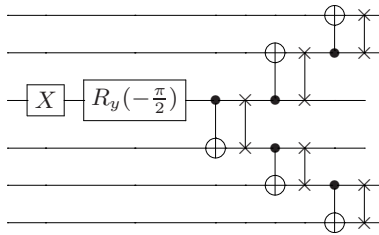


FIG. 3: A quantum circuit to entangle all qubits in a quantum register in a GHZ state. In this figure, the CNS gates are represented by a directed CNOT gate followed by a SWAP gate.

creating a so-called GHZ state [17]:

$$|\text{GHZ}\rangle = \frac{|0\rangle^{\otimes N} + |1\rangle^{\otimes N}}{\sqrt{2}}. \quad (14)$$

For a 6-qubit chain, we arrive at the gate sequence depicted in Fig. 3. In this sequence, some of the CNS gates can be applied in parallel. Also, during the gate operation, the remaining qubits need to be decoupled from their neighbors. To achieve this, we can use a combined decoupling sequence as presented in Sec. III C.

We conducted numerical simulations for this gate sequence by calculating the resulting state $|\Psi\rangle$, where we assume that all qubits are initially in the state $|0\rangle$. We calculated the fidelity \mathcal{F}_{GHZ} of the GHZ state depending on the pulse amplitude f ,

$$\mathcal{F}_{\text{GHZ}} = |\langle \text{GHZ} | \Psi \rangle|. \quad (15)$$

We simulated qubit chains of up to 8 qubits for pulse amplitudes of $f = 20g$, $f = 40g$, $f = 60g$ and $f = 80g$. For $f = 20g$ and $f = 40g$, the basic decoupling sequence with four operations was used, for $f = 60g$ and $f = 80g$ the symmetrized decoupling scheme with eight operations was used. The results are shown in table I. As we can see, a pulse amplitude of $f = 20g$ is sufficient to entangle 3 qubits, however, the fidelity falls very quickly with increasing number N of qubits. In contrast, a pulse amplitude of $f \geq 40g$ can be used to entangle even 8 qubits with high fidelity.

The results in table I were achieved under the assumption that the qubits' eigenenergies are all the same, meaning that the Δ_i in Eq. (2) are all zero. Non-zero Δ_i have a detrimental effect on the achievable fidelity. However, our decoupling scheme offers limited robustness against these effects, as long as the Δ_i are small compared to the pulse amplitude. We ran additional simulations where we sampled the Δ_i randomly from a Gaussian distribution with mean value $\mu = 0$ and standard deviation σ . Results of the achievable fidelity, averaged over 100 runs, depending on σ are plotted in Fig. 4 for a chain of four qubits. We can see that the drop in the averaged fidelity is acceptable if σ is not too large and is smaller

N	$f = 20g$	$f = 40g$	$f = 60g$	$f = 80g$
3	0.900	0.969	0.974	0.985
4	0.779	0.927	0.949	0.969
5	0.697	0.894	0.932	0.958
6	0.616	0.860	0.915	0.948
7	0.540	0.821	0.896	0.935
8	0.503	0.796	0.876	0.922

TABLE I: Numerical simulation results for the achievable fidelity of the GHZ state, depending on the number N of qubits and the pulse amplitude f .

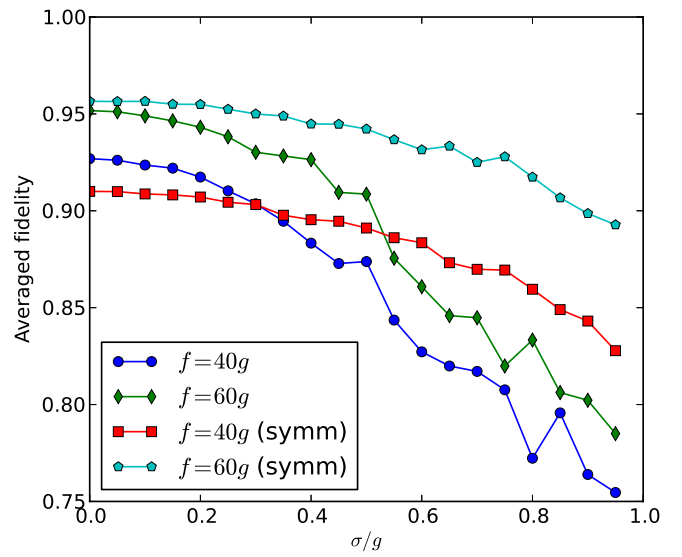


FIG. 4: (Color online) Averaged fidelity for a GHZ state achievable on a 4-qubit chain for different values of the pulse amplitude f , when the qubit eigenenergies differ from each other. The Δ_i are randomly sampled from a Gaussian distribution with standard deviation σ . With increasing σ , the achievable fidelity drops. The plotted results were averaged over 100 runs.

than the coupling g . The symmetric decoupling scheme is particularly robust against errors and outperforms the basic scheme at larger σ values. We can expect that with improved manufacturing processes the qubit eigenenergy discrepancies will become sufficiently small in the future so that the resulting inhomogeneous broadening is negligible.

VI. CONCLUSIONS

We presented a coupled qubit system modelled after superconducting flux qubits which is fully controlled by a pulse generator. The qubits are strongly coupled to their neighbours, and the coupling is always present. We demonstrated how the pulse generator can be used to

implement both single-qubit rotations and the two-qubit entangling CNS gate. For the implementation of the two-qubit gate we exploit the coupling between the qubits and use a dynamical decoupling scheme to decouple the gate qubits from the remaining qubits in the system. The decoupling scheme is flexible so that several two-qubit gates can be implemented in parallel.

The efficiency of our control scheme was analyzed in numerical simulations, where we first looked at a single gate application. Then a sequence of CNS gates was simulated to entangle all the qubits in the chain in a GHZ state. In both cases, we calculated the achievable fidelity based on the pulse amplitude of the pulse generator. We found that a fidelity of well over 0.9 is achievable for a single CNS gate operation. In order to entangle N qubits in a GHZ state, $N-1$ CNS gates are required. Since additionally all the other qubits have to be decoupled during gate operations, the fidelity for the GHZ state directly depends on the number of qubits in the chain. In order to compensate for this effect, the pulse amplitude needs to be increased. However, this is physically limited by the energy gap to higher excited states, which should not be excited by the pulse generator. Taking this limit into ac-

count for the particular example of flux qubits, we find that a high fidelity for the GHZ state is only achievable for a relatively small number of qubits, unless the coupling strength between the qubits is reduced. Employing more sophisticated pulse shapes may help to surpass this limit.

In order to achieve true scalability, error correction will be required. De and Pryadko recently demonstrated how a universal set of quantum gates could be implemented on a qubit lattice with Ising couplings [42]. They then implemented the toric code on top of this lattice to achieve scalability [43]. We believe that this approach could be adopted in principle for our model.

Acknowledgments

The authors acknowledge financial support by CASEDIII and by the BMBF-project Q.com. This work has been co-funded by the DFG as part of project S4 within the CRC 1119 CROSSING.

[1] M. Schlosser, S. Tichelmann, J. Kruse, and G. Birk, Quant. Inf. P. **10**, 907 (2011).

[2] M. Anderlini, P. J. Lee, B. L. Brown, J. Sebby-Strabley, W. D. Phillips, and J. V. Porto, Nature **448**, 452 (2007).

[3] T. Wilk, A. Gaetan, C. Evellin, J. Wolters, Y. Miroshnychenko, P. Grangier, and A. Browaeys, Phys. Rev. Lett. **104**, 010502 (2010).

[4] L. Isenhower, E. Urban, X. L. Zhang, A. T. Gill, T. Henage, T. A. Johnson, T. G. Walker, M. Saffman, Phys. Rev. Lett. **104**, 010503 (2010).

[5] J. T. Muhonen, J. P. Dehollain, A. Laucht, F. E. Hudson, R. Kalra, T. Sekiguchi, K. M. Itoh, D. N. Jamieson, J. C. McCallum, A. S. Dzurak, and A. Morello, Nat. Nano. **10**, 1038 (2014).

[6] N. Zhao, J. Honert, B. Schmid, M. Klas, J. Isoya, M. Markham, D. Twitchen, F. Jelezko, R.-B. Liu, H. Fedder and J. Wrachtrup, Nat. Nano. **7**, 657 (2012).

[7] I. Buluta, S. Ashhab, and F. Nori, Rep. Prog. Phys. **74**, 104401 (2011).

[8] M. H. Devoret and R. J. Schoelkopf, Science **339**, 1169 (2013).

[9] D. D. Awschalom, L. C. Bassett, A. S. Dzurak, E. L. Hu, and J. R. Petta, Science **8**, 1174 (2013).

[10] H. Bluhm, S. Foletti, I. Neder, M. Rudner, D. Mahalu, V. Umansky, and A. Yacoby, Nat. Phys. **7**, 109 (2011).

[11] P.-Q. Jin, M. Marthaler, A. Shnirman, and G. Schon, Phys. Rev. Lett. **108**, 190506 (2012).

[12] M. D. Shulman, O. E. Dial, S. P. Harvey, H. Bluhm, V. Umansky, and A. Yacoby, Science **336**, 202 (2012).

[13] L. DiCarlo, M. D. Reed, L. Sun, B. R. Johnson, J. M. Chow, J. M. Gambetta, L. Frunzio, S. M. Girvin, M. H. Devoret, and R. J. Schoelkopf, Nature **467**, 574 (2010).

[14] M. Steffen, M. Ansmann, R. C. Bialczak, N. Katz, E. Lucero, R. McDermott, M. Neeley, E. M. Weig, A. N. Cleland, and J. M. Martinis, Science **8**, 1423 (2006).

[15] M. Stern, G. Catelani, Y. Kubo, C. Grezes, A. Bienfait, D. Vion, D. Esteve, and P. Bertet, Phys. Rev. Lett. **113**, 123601 (2014).

[16] J. B. Majer, F. G. Paauw, A.C.J. ter Haar, C. J. P.M. Harmans, and J. E. Mooij, Phys. Rev. Lett. **94**, 090501 (2005).

[17] D. Greenberger, M. Horne, and A. Zeilinger, arXiv:0712.0921 (2007).

[18] L. Viola, E. Knill, and S. Lloyd, Phys. Rev. Lett. **82**, 2417 (1999).

[19] E. L. Hahn, Phys. Rev. **80**, 580 (1950).

[20] H. Y. Carr and E. M. Purcell, Phys. Rev. **94**, 630 (1954).

[21] S. Meiboom and D. Gill, Rev. Sci. Instrum. **29**, 688 (1958).

[22] Ü. Haeberlen, *High Resolution NMR in Solids* (Waltham: Academic Press, 1976).

[23] J. J. L. Morton, A. M. Tyryshkin, A. Ardavan, S. C. Benjamin, K. Porfyrakis, S. A. Lyon, and G. A. D. Briggs, Nat. Phys. **2**, 40 (2006).

[24] E. Fraval, M. J. Sellars, and J. J. Longdell, Phys. Rev. Lett. **95**, 030506 (2005).

[25] M. J. Biercuk, H. Uys, A. P. Van Devender, N. Shiga, W. M. Itano, and J. J. Bollinger, Nature (London) **458**, 996 (2009).

[26] M. Lucamarini, G. Di Giuseppe, S. Damodarakurup, D. Vitali, and P. Tombesi, Phys. Rev. A **83**, 032320 (2011).

[27] G. Heinze, C. Hubrich, and T. Halfmann, Phys. Rev. Lett. **111**, 033601 (2013).

[28] L. Viola, S. Lloyd, and E. Knill, Phys. Rev. Lett. **83**, 4888 (1999).

[29] M. Stollsteimer and G. Mahler, Phys. Rev. A **64**, 052301 (2001).

[30] D. Leung, J. Mod. Opt. **49**, 1199 (2002).

- [31] M. Rötteler and P. Wocjan, IEEE Trans. Inf. Theory **52**, 4171 (2006).
- [32] P. Wocjan, M. Rötteler, D. Janzing, and T. Beth, Phys. Rev. A **65**, 042309 (2002).
- [33] H. Frydrych, G. Alber, and P. Bažant, Phys. Rev. A **89**, 022320 (2014).
- [34] W. Magnus, Comm. Pure and Appl. Math. **VII**, 649 (1954).
- [35] D. P. Burum, Phys. Rev. B **24**, 3684 (1981)
- [36] N. Schuch and J. Siewert, Phys. Rev. A. **67**, 032301 (2003).
- [37] L. Viola and E. Knill, Phys. Rev. Lett. **90**, 037901 (2003).
- [38] O. Kern and G. Alber, Phys. Rev. Lett. **95**, 250501 (2005).
- [39] Yu Chen, C. Neill, P. Roushan, N. Leung, M. Fang, R. Barends, J. Kelly, B. Campbell, Z. Chen, B. Chiaro, A. Dunsworth, E. Jeffrey, A. Megrant, J. Y. Mutus, P. J. J. O’Malley, C. M. Quintana, D. Sank, A. Vainsencher, J. Wenner, T. C. White, Michael R. Geller, A. N. Cleland, and J. M. Martinis, arXiv:1402.7367 (2014).
- [40] L. P. Pryadko and P. Sengupta, Phys. Rev. A **78**, 032336 (2008).
- [41] F. Motzoi and F. K. Wilhelm, Phys. Rev. A **88**, 062318 (2013).
- [42] A. De and L. P. Pryadko, Phys. Rev. Lett. **110**, 070503 (2013).
- [43] A. De and L. P. Pryadko, Phys. Rev. A **89**, 032332 (2014).